

# Improvement in Sensing Response of Nano-Crystalline ZnO based Hydrogen Sensor: Effect of Swift Heavy Ion Irradiation

In advancement for enhancing sensors response, various surface modulation technique has been used. Here, we have focused on post deposition techniques like swift heavy ion irradiation. Nano-crystalline ZnO thin films has been irradiated using 120 MeV Au<sup>+9</sup> ions at various ion fluences. Structural, optical and surface morphology have been altered with incremental ion fluences causing change in hydrogen gas sensor's response to large extent. In addition, improvement in sensor's response have been achieved by grain fragmentation generated by swift heavy ions. And the relative change in sensor's response at different operating temperatures and ion fluences have also been indicated.

## 8.1 INTRODUCTION

Thin film and nanostructures based gas sensor's key parameters such as sensitivity (relative response), response/recovery time and operating temperature can be enhanced by surface modulation techniques. Surface modification can be done by adding catalysts or variation of deposition parameters or post deposition treatment. Practically, post deposition treatments such as annealing and swift heavy ion (SHI) irradiation bring vast changes in materials properties [Agerwal *et al.*, 2008; Neogi *et al.*, 2011].

SHI irradiation is a powerful technique to alter structural properties and surface morphology of the material, which can enhance gas-sensing properties [Mene *et al.*, 2011]. Furthermore, in-plane stress in nano-crystalline thin film can also affect optical, structural and electrical properties to a large extent [Ghosh *et al.*, 2004]. Due to lattice and thermal expansion coefficient mismatch between film material and substrate, deposition parameters generate in-plane stress, which can be modified by SHI irradiation [Rao *et al.*, 2009]. The stress can also vary the optical band gap of ZnO thin film [Singh *et al.*, 2015]. In-plane stress generation in ZnO thin film is observed due to incremental ion fluences of 120 MeV Ag<sup>+9</sup> ion irradiation in [Singh *et al.*, 2010]. However, gas sensor application is basically based on surface reaction of target gas and sensing thin films and nanostructures. When high energy ion passes through a target material, two kinds of energy losses take place firstly nuclear energy loss ( $S_n$ ) due to elastic collision which transfers direct energy to target atoms. Secondly electronic energy loss ( $S_e$ ) due to inelastic collision which causes electronic ionization of target atoms [Sharma *et al.*, 2011]. In SHI irradiation, electronic energy loss is of several orders higher than nuclear energy loss. When each SHI passes through target material, it produces perturbation in the electronic system of the target material in a narrow cylindrical path along its trajectory due to high inelastic collision between SHI and target material. These SHI induces variety of defects and local heating along its trajectory, which plays an important role in thin film gas sensors due to surface modification and change in electrical transport properties [Sagade *et al.*, 2009; Agerwal *et al.*, 2008]. Surface morphology's basic parameters such as roughness, fractal dimension and PSD (power spectral density) are enough to understand SHI irradiation effects on surface engineering where fractal dimension and PSD parameters are based on scaling concepts [Dallaeva *et al.*, 2008; Roufi *et al.*,

2010]. Fractal characterization helps to explain change in dynamics of surface roughness. Yadav *et al.* in [Yadav *et al.*, 2015], studied fractal and multi fractal characterization of self-affine surfaces of BaF<sub>2</sub> thin films with 120 MeV Ag<sup>9+</sup> ion fluence, which also contributed to change in surface morphology. When high energy ion passes through thin films, electron-lattice interaction increases energy along the ion tracks and causes internal strain and fragmentation of these thin film structures [Agerwal *et al.*, 2008]. Sagade *et al.* in [Sagade *et al.*, 2009], studied effect of 100 MeV gold SHI irradiation on Cu<sub>x</sub>S thin films and found change in surface morphology and improvement in ammonia gas detection. Mane *et al.* in [Mane *et al.*, 2011], analysed the effect of 100 MeV Ag<sup>7+</sup> ions on hydroxyapatite (HAp) thick film based CO gas sensor and authenticated the enhancement in gas response and fast response/recovery time with irradiation at 195°C. Balkrishnan *et al.* in [Balkrishnan *et al.*, 2015] enhanced ZnO thin film based ammonia gas sensor's sensitivity and response time by Ag ion fluences where morphology of thin films transforms into needle like shapes with high roughness as ion fluence increases. Here, we have concentrated on the effects of SHI irradiation on structural, surface morphology, optical and hydrogen gas sensing properties of nano-crystalline ZnO thin films.

## 8.2 EXPERIMENTAL SETUP

ZnO thin films of ~300 nm were deposited on p-type Si (100) substrate using RF sputtering technique. ZnO target (99.999 % purity) was used for deposition with chamber base pressure of 1x10<sup>-6</sup> mbar. Highly pure mixture of Ar: O<sub>2</sub> was used with constant gas flow of 28 sccm: 11.5 sccm to create plasma. RF power, target to substrate distance, substrate temperature and chamber pressure were maintained at 150 W, 15 cm, room temperature and 2x10<sup>-2</sup> mbar, respectively. These samples were irradiated with 120 MeV Au ions at incremental ion fluences varying from 1x10<sup>11</sup> to 1x10<sup>13</sup> ions/cm<sup>2</sup> using 15UD pelletron tandem accelerator at the Inter-University Accelerator Centre (IUAC), New Delhi. To achieve uniform irradiation throughout ZnO thin film surface, ion beam was scanned over 1x1 cm<sup>2</sup> area and beam current was maintained at ~0.5 particles nano ampere (pnA). Angle of incidence of ion beam was kept 90° to the samples. The electronic energy loss (S<sub>e</sub>) for 120 MeV Au ions in ZnO was 18.84 keV/nm while nuclear energy loss (S<sub>n</sub>) was 0.34 keV/nm and penetration range was ~ 12.90 μm as calculated using the SRIM simulation code.

Aluminium contacts were deposited by thermal deposition technique using physical mask with circular dots of 400 μm diameter and 3.2 mm spacing. Contact of 150 nm thickness was taken. Gas sensor characterization was carried out in a vacuum chamber where base pressure was maintained at ~2x10<sup>-3</sup> mbar. Thin film sensor's operating temperature was varied from 75 °C to 175 °C using an external heater. The gas sensing measurements were performed in presence of 5% hydrogen in argon concentration. Gas sensor response was measured in form of film resistance that varies with respect to time at operating temperatures ranging between 75 °C to 175 °C. Table 8.1 shows nano crystalline ZnO thin film optimization parameters and SHI gas sensing parameters.

**Table 8.1:** Deposition, SHI irradiation and gas sensing parameters for nano-crystalline ZnO thin film based nanosensor

Substrate	2 inch p-Si (100)
Sputtering target	ZnO (99.999% purity)
Base pressure	1x10 <sup>-6</sup> mbar
Deposition pressure	2x10 <sup>-2</sup> mbar
Deposition time	2 hour
RF power	150 W
Sputtering gas	Argon (28 sccm):oxygen (11.5 sccm)
Substrate temperature	RT
Target to substrate distance	15 cm

Metallization technique	Thermal evaporation
Metal contact	Al (400 $\mu\text{m}$ diameter, 150 nm thickness) Spacing between two metal contact~3.2mm
SHI irradiation	120 MeV Au <sup>9</sup>
Ion beam current	0.5 partial nano Ampere (pnA)
SHI ion fluences	$1 \times 10^{11}$ ions/cm <sup>2</sup> , $1 \times 10^{12}$ ions/cm <sup>2</sup> , $1 \times 10^{13}$ ions/cm <sup>2</sup>
Gas sensor operating temperature	75 °C to 175 °C
Hydrogen concentration	5% (in pure argon)

### 8.3 STRUCTURAL PROPERTIES OF NANO-STRUCTURE ZnO THIN FILMS

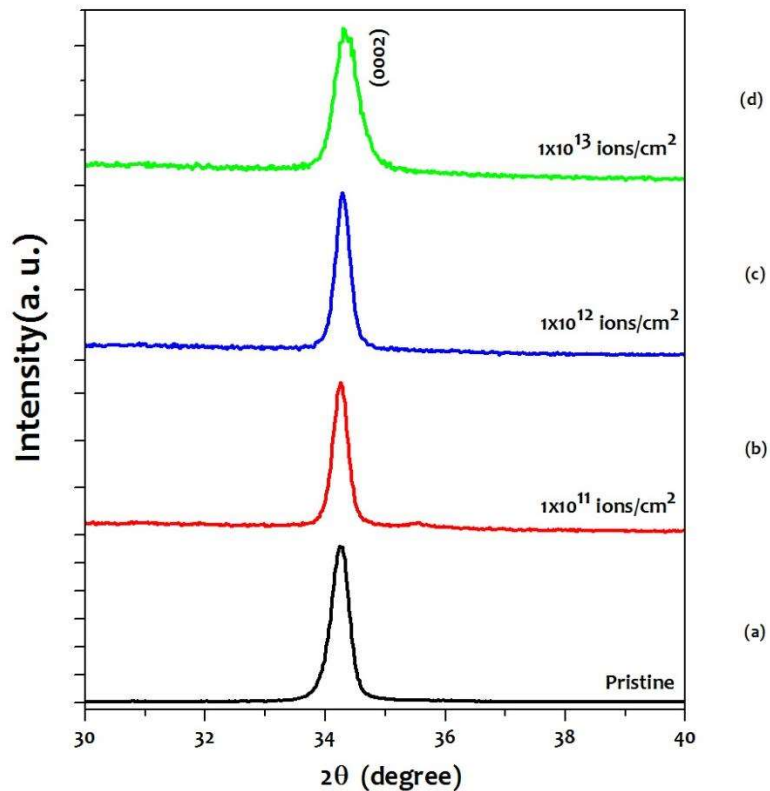


**Figure 8.1:**  $2\theta$ - $\omega$  Scan of XRD spectra of nano crystalline ZnO thin films: (a) Un-irradiated (pristine), and irradiated at ion fluences of (b)  $1 \times 10^{11}$  ions/cm<sup>2</sup>, (c)  $1 \times 10^{12}$  ions/cm<sup>2</sup> and (d)  $1 \times 10^{13}$  ions/cm<sup>2</sup>

The structural characterization of pristine and 120 MeV Au SHI irradiated films at various fluences were performed by XRD. Figure 8.1 shows  $2\theta$ - $\omega$  scan of XRD spectra of pristine and irradiated nano crystalline ZnO thin film at different ion fluences. XRD spectra shows single (0002) diffraction peak at  $34.24^\circ$  for pristine ZnO thin film indicating that ZnO thin films are highly crystalline, c-oriented and wurtzite in crystal structure [Ranwa *et al.*, 2015]. Shift in (0002) peak position towards higher diffraction angle with incremental ion fluences in irradiated film was also observed in comparison to pristine thin film. When thin film was irradiated with increasing ion fluences up to  $1 \times 10^{12}$  ions/cm<sup>2</sup>, (0002) peak full width half maximum (FWHM) almost constant in compared to pristine sample. Figure 8.2 shows variation in FWHM with increasing ion fluences. Lesser change in FWHM indicates that crystallinity of ZnO thin film almost constant. At low fluences, ions in single track removes strain between ZnO grains and

provide local heating resulting in improved crystalline thin film when compared with pristine ZnO thin film. At higher fluences of  $1 \times 10^{13}$  ions/cm<sup>2</sup>, FWHM was increased and the crystallinity of ZnO thin film was degraded because high fluences promoted dense electronic excitation which lead to overlapping of track that further stimulated lattice disorder within the grain and at grain boundaries, resulting in reduced crystalline order of the film [Agerwal *et al.*, 2006].

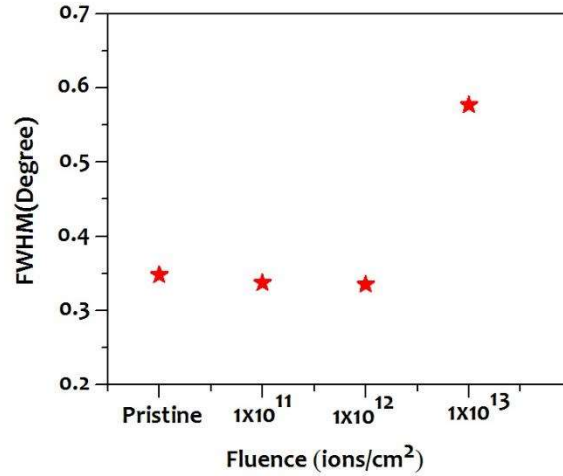


**Figure 8.2:** Variation of FWHM with ion fluence at increasing rate from  $1 \times 10^{11}$  ions/cm<sup>2</sup> to  $1 \times 10^{13}$  ions/cm<sup>2</sup>

### 8.4 STRESS ANALYSIS

Additionally, In-plane stress in thin film can be evaluated from XRD diffraction using following equation [Singh *et al.*, 2010]:

$$\sigma(Pa) = -233 \times 10^9 \left[ \frac{c - c_0}{c_0} \right] \tag{8.1}$$

where  $\sigma$  is the in-plane stress and  $c$  and  $c_0$  are lattice constant and stress free lattice constant ( $\sim 5.206 \text{ \AA}$ ) for ZnO thin film, respectively. The lattice constant can be calculated from XRD pattern. Figure 8.3 shows change in compressive stress with variation of ion fluences. It is observed that pristine ZnO thin film has high compressive stress of  $-1.78 \text{ GPa}$ , which is inversely proportional to ion fluences and ZnO film becomes almost stress free at ion fluences of  $1 \times 10^{13}$  ions/cm<sup>2</sup>. Due to high energy ion irradiation at highest fluences, ions track generates local heating and annealing effect which reduces in-plane stress in thin films in comparison to un-irradiated thin films. Therefore, in-plane stress can be minimized with the help of such effects.

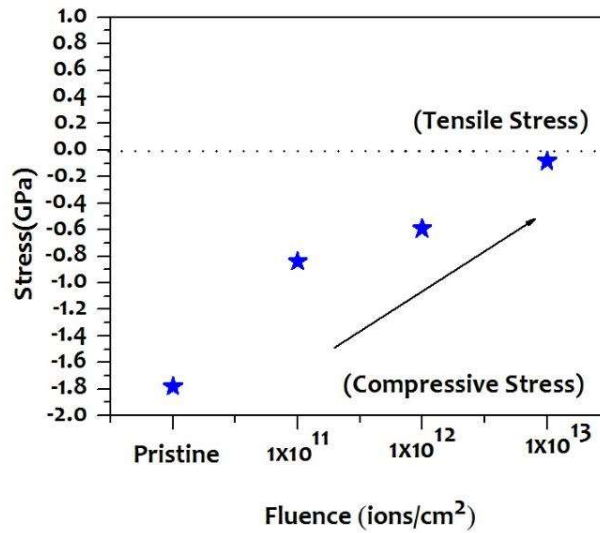


**Figure 8.3 :** Variation of compressive stress with ion fluences at increasing rate from  $1 \times 10^{11}$  ions/cm<sup>2</sup> to  $1 \times 10^{13}$  ions/cm<sup>2</sup>

## 8.5 OPTICAL PROPERTIES OF NANO-STRUCTURE ZnO THIN FILMS

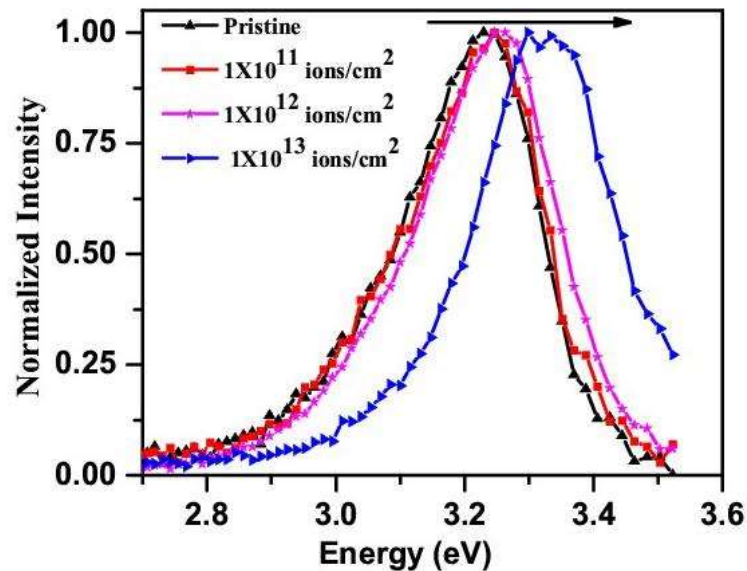


**Figure 8.4 :** Normalized CL spectra of pristine and irradiated ZnO thin films at room temperature

Effect of SHI on CL emission have also been explored. Figure 8.4 shows normalized CL spectra of pristine and SHI irradiated ZnO thin films at room temperature. Pristine ZnO thin film gives strong near band emission (NBE) peak at 3.23 eV with  $\sim 0.22$  eV peak width [Kumar *et al.*, 2012]. A blue shift in NBE peak from 3.23 eV to 3.33 eV in CL spectra can be spotted as ion fluence increases up to  $1 \times 10^{13}$  ions/cm<sup>2</sup>. NBE peak shifts towards higher energy region due to reduction of in-plane compressive stress with increasing ion fluences [Singh *et al.*, 2015].

## 8.6 EFFECT OF SHI ON SURFACE MORPHOLOGY

Effects of SHI irradiation on surface morphology were studied using AFM. Figure 8.5 (a), (b), (c) and (d) shows AFM 2-D images of pristine and irradiated samples with various fluences ( $1 \times 10^{11}$  ions/cm<sup>2</sup> to  $1 \times 10^{13}$  ions/cm<sup>2</sup>) of Au<sup>+9</sup> ions. Surface morphology of pristine ZnO thin film shows uniform distribution of spherical grains of ZnO throughout the surface.

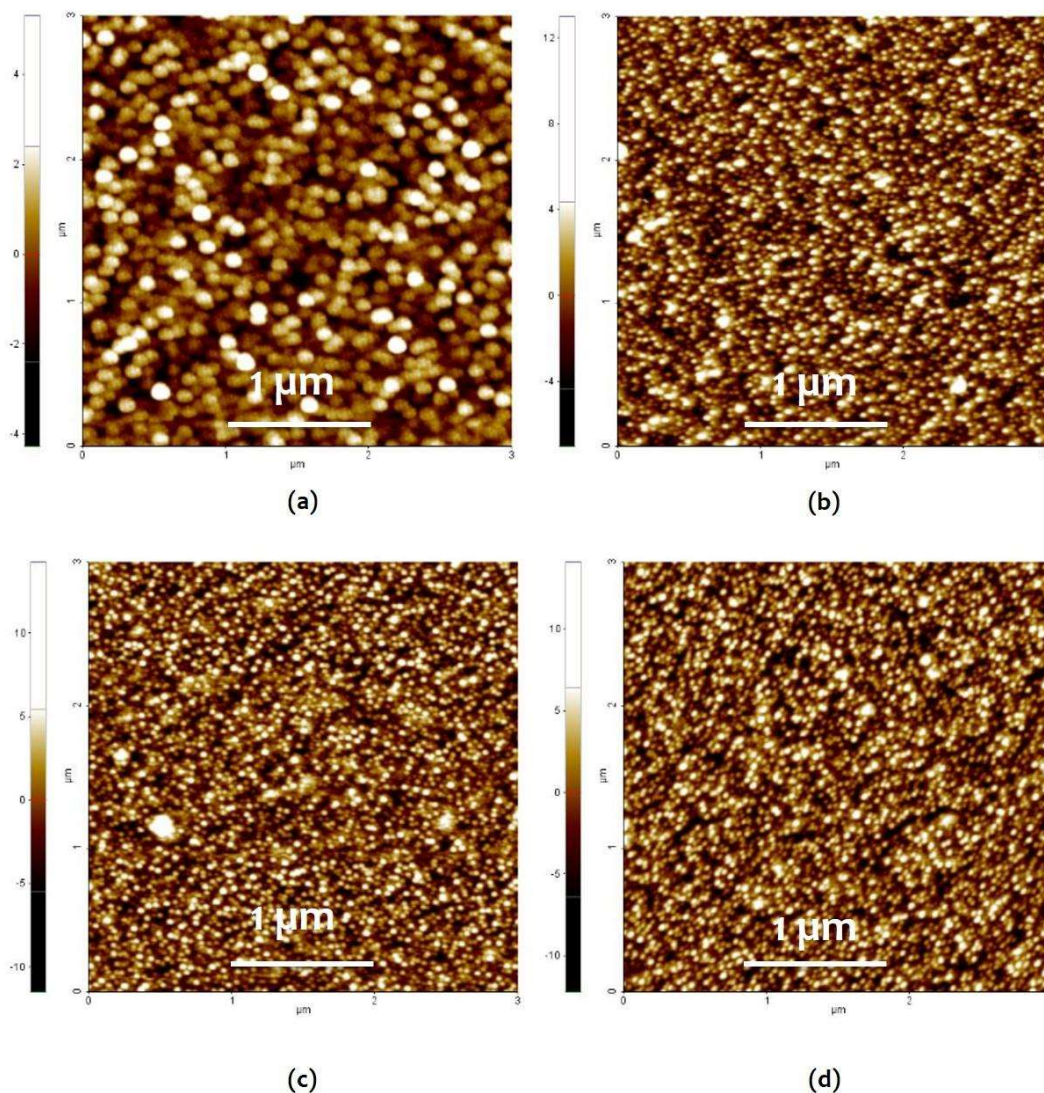


**Figure 8.5 :** AFM 2-D images of ZnO thin films: (a) Pristine (un-Irradiated), irradiated at (b)  $1 \times 10^{11}$  ions/cm<sup>2</sup>, (c)  $1 \times 10^{12}$  ions/cm<sup>2</sup>, (d)  $1 \times 10^{13}$  ions/cm<sup>2</sup> fluences of Au ions, respectively

RMS roughness of  $\sim 1.22$  nm and average grain size of  $\sim 145$  nm were calculated by XEI AFM software. Average grain size of 108.5 nm, 96.5 nm and 91.1 nm were obtained for spherical nanostructure at ion fluences of  $1 \times 10^{11}$  ions/cm<sup>2</sup>,  $1 \times 10^{12}$  ions/cm<sup>2</sup> and  $1 \times 10^{13}$  ions/cm<sup>2</sup>, respectively. Surface roughness and density of ZnO grains also increased with ion fluences. Besides, SEM characterization also supported AFM results. Figure 8.6 (a) and (b) shows SEM images of nano-crystalline ZnO thin film of pristine and  $1 \times 10^{13}$  ions/cm<sup>2</sup> irradiation samples, respectively. SEM image shows dark halos throughout the film irradiated with  $1 \times 10^{13}$  ions/cm<sup>2</sup> fluences, which indicates that the crystallinity of thin film reduces as validated by previous XRD results.

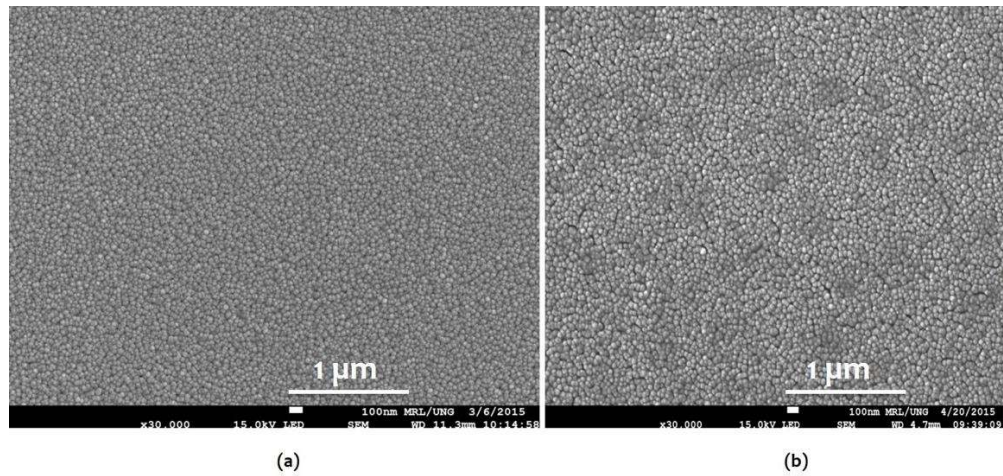


**Figure 8.6 :** Top view SEM images for (a) Pristine and (b)  $1 \times 10^{13}$  ions/cm<sup>2</sup> Au SHI irradiated ZnO thin film

This proves that surface modulation can be accomplished by high energy ions as they change surface energy in near surface region [Agerwal *et al.*, 2009]. High energy ion beam generates strain in ZnO grains as defined by thermal spike model [Volkov and Borodin, 2002]. According to this model, initially, heavy ions deposit energy to electronic subsystem of target, which is then transferred to lattice atom and due to this transferred energy to lattice atom, temperature increases along ion path and causes strain in ZnO grains, and the internally generated strain leads to fragmentation of ZnO grains [Agerwal *et al.*, 2008]. RMS roughness and surface scaling analysis like PSD and fractal analysis provides comprehensive information about the surface modification. Figure 8.7 shows (a) 2D PSD vs spatial frequency of ZnO thin film surfaces and (b) RMS roughness and fractal dimension variation at different ion fluences. Power spectral density (PSD) is independent of scan size and provides information about quantitative surface roughness. The fractal surface maintains the characteristics of continuity and self-similarity of ZnO nanostructures [Yadav *et al.*, 2015]. In this work, correlation between fractal dimension and RMS roughness is discussed where both increases with ion fluences. PSD always follow inverse power law with spatial frequency and displays the presence of fractal component in the surface morphology [Yadav *et al.*, 2015]. The slope of PSD curve in high frequency region increases with fluence. Roughness exponent's ( $\alpha = (\gamma - 2)/2$ , where  $\gamma$  indicate slope of PSD curve) calculated value lies between 0 to 1 that confirms the formation of self-affine fractal surface due to SHI fluences.

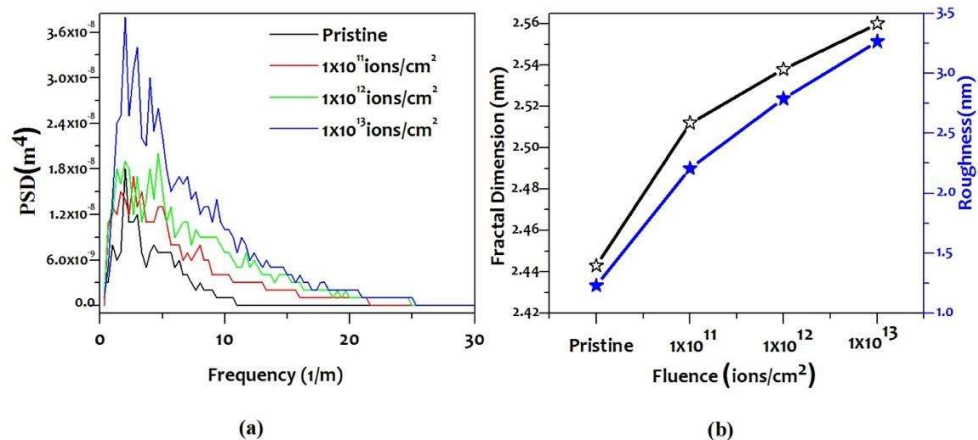


**Figure 8.7 :** (a) 2D PSD plot v/s spatial frequency and (b) RMS roughness and fractal dimension variation at different ion fluences, respectively

## 8.7 EFFECT OF SHI ON HYDROGEN GAS NANO-SENSOR

Study of hydrogen gas sensing for pristine and irradiated ZnO thin films was carried out for 5% hydrogen concentration. Effect of SHI irradiation on gas sensing parameters such as sensitivity, response/recovery time was studied at various operating temperatures from 75°C to 175 °C. Gas sensor's relative response can be defined as  $\Delta R/R_a$ , where  $\Delta R = |R_a - R_g|$ ,  $R_a$  and  $R_g$  are sensor resistance in air and reactive gas, respectively [Oh *et al.*, 2009; Pawar *et al.*, 2013]. Gas sensing always depends on adsorbed reactive gas and operating temperature. Gas sensing mechanism is basically defined in terms of adsorption/desorption of reactive gases on sensing material surfaces where conductivity of thin film can be altered by capturing/releasing conduction band electrons. Defects and chemisorbed reaction of oxygen at grain boundaries leads to change in film's resistance. When nano-crystalline ZnO thin film gets exposed to environmental oxygen, absorbed oxygen captures electron from conduction band of thin film and film resistance increases due to formation of depletion region. Thus, change in film resistance basically depends on absorbed oxygen ions ( $O^-$ ,  $O^{2-}$  etc.) and defects and acts as trapping centre for oxygen molecules.

During hydrogen loading, oxygen ions react with hydrogen molecules and release electrons in conduction band of thin film, which increases film conductivity. These reactions are exothermic and water molecules are also desorbed from surface. Figure 8.8 (a), (b), (c) and (d) represents temperature dependent resistive response curve for 5% hydrogen concentration on pristine and irradiated ZnO thin film with 120 MeV Au at ion fluences of  $1 \times 10^{11}$  ions/cm<sup>2</sup>,  $1 \times 10^{12}$  ions/cm<sup>2</sup> and  $1 \times 10^{13}$  ions/cm<sup>2</sup>, respectively. As operating temperature increases from 75 °C to 175 °C with incremental steps of 50 °C, rate of adsorption/desorption of reactive gases increases.

Hydrogen gas sensor's response curve is highly influenced by surface modification and sensor operating temperature. In pristine and irradiated nano-crystalline ZnO thin film, as operating temperature is increased from 75 °C to 175 °C, change in film's resistance is more in presence of hydrogen gas as compared to air.

High energy ions modify grain boundaries and reduces average grain size which provides larger surface reaction area for hydrogen gas, which, as a result, enhances sensing response. This enhancement in adsorption/desorption reaction is due to reduction in average grain size that provides larger reactive surface and improved crystallinity that attributes to high electric conductivity. Figure 8.8 (d) shows less change in resistive response curve at various operating temperatures in comparison to pristine nano crystalline ZnO thin film because of reduction in crystallinity.



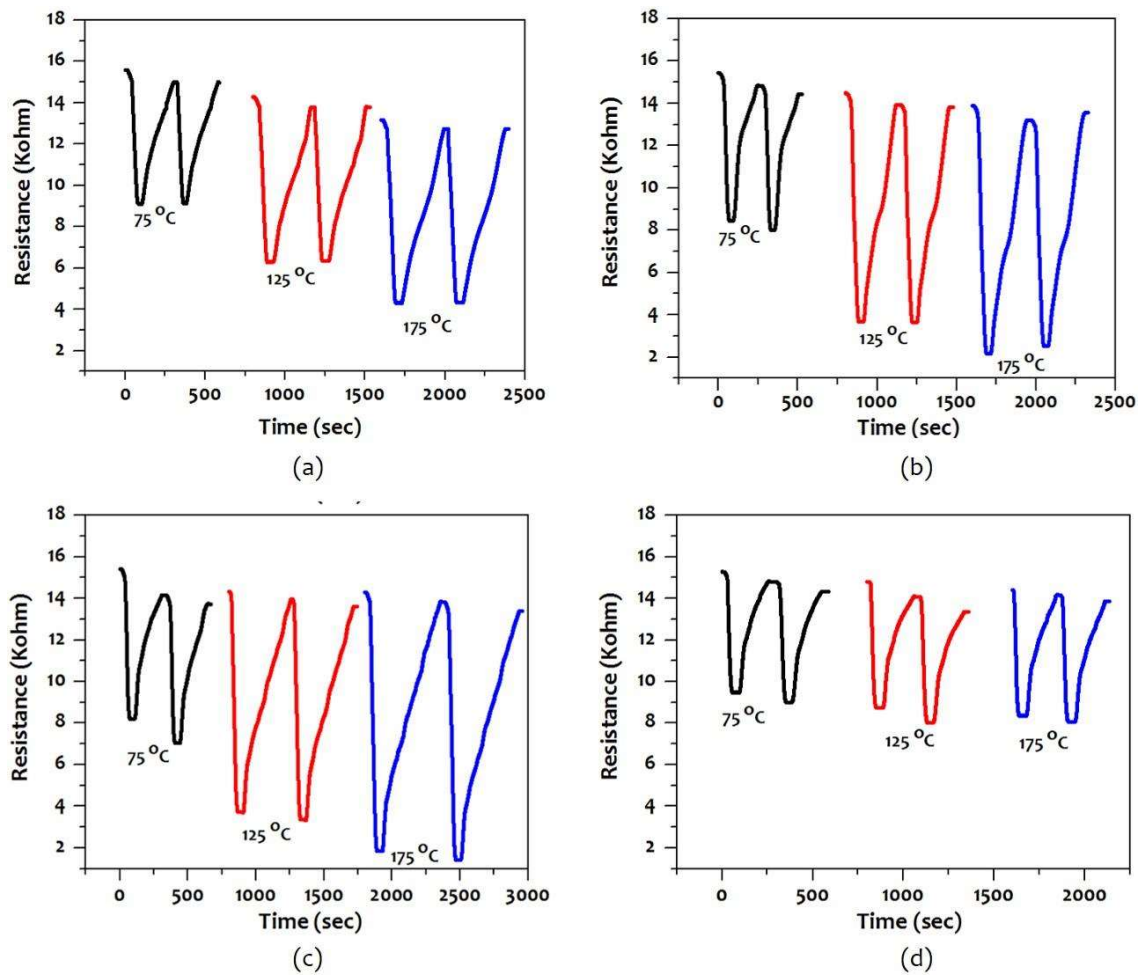


**Figure 8.8 :** Temperature dependent resistive response curve for 5% hydrogen concentration on (a) Pristine, and irradiated ZnO thin film with 120 MeV Au at ion fluences of (b)  $1 \times 10^{11}$  ions/cm<sup>2</sup>, (c)  $1 \times 10^{12}$  ions/cm<sup>2</sup> and (d)  $1 \times 10^{13}$  ions/cm<sup>2</sup>, respectively

Modification of relative response of ZnO thin film sensor with various ion fluences for 75 °C to 175 °C operating temperature has been shown in Figure 8.9. For pristine ZnO thin film, sensitivity varies from 41.69% to 66.68% as operating temperature is varied from 75 °C to 175 °C. Because of high crystallinity of ZnO thin film and its nano scale grain boundaries, sensitivity is improved even at low operating temperature range (<200 °C) in ZnO film based hydrogen sensors. As ion fluence increases from  $1 \times 10^{11}$  ions/cm<sup>2</sup> to  $1 \times 10^{13}$  ions/cm<sup>2</sup>, change in gas sensor's relative response increases with increase in the operating temperature. SHI reduces average grain size that enhances reaction rate by increasing surface to volume ratio. Thus, XRD and AFM results confirms that sensitivity increases as average grain size reduces and film's crystallinity enhances with incremental ion fluence from  $1 \times 10^{11}$  ions/cm<sup>2</sup> to  $1 \times 10^{13}$  ions/cm<sup>2</sup>. With various ion fluences, sensitivity is boosted from 66.68% to 89.84% for operating temperature of 175°C.

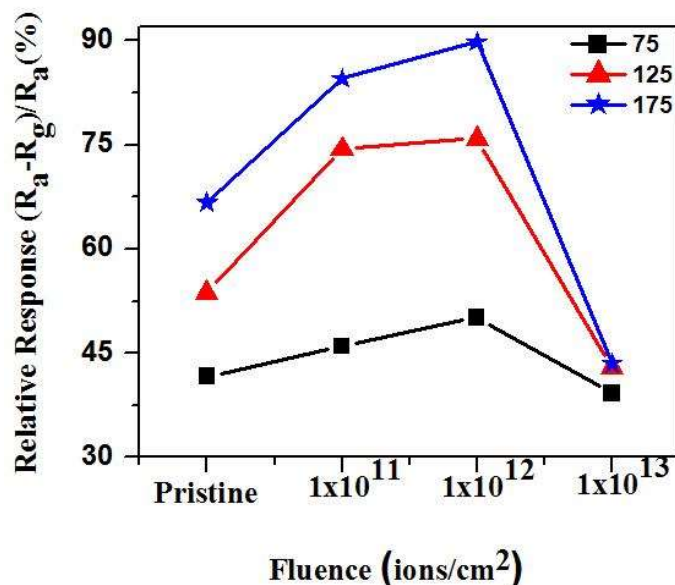


**Figure 8.9:** Relative response variation of ZnO thin film sensor with various ion fluences for 75 °C to 175 °C operating temperature

Response and recovery time were calculated by  $T = |t_{90\%} - t_{10\%}|$  where  $t_{90\%}$  and  $t_{10\%}$  is the time required to reach 10% and 90% of maximum resistive response value [Park and Oh, 2009]. Calculated response and recovery time with various ion fluences and operating temperature between 75 °C to 175 °C are listed in Table 8.2. ZnO thin film based hydrogen sensor gives maximum sensitivity of 89.84%, fast response of ~34.67 sec. and moderate recovery time of ~346.74 sec. at 175 °C with fluence  $1 \times 10^{12}$  ions/cm<sup>2</sup>.

**Table 8.2 :** Estimated response and recovery time of ZnO thin film based gas sensor exposed at various ion fluencies at different operating temperatures (75 °C to 175 °C)

	Response time (75 °C)	Recovery time (75 °C)	Response time (125 °C)	Recovery time (125 °C)	Response time (175 °C)	Recovery time (175 °C)
<b>Pristine</b>	14 sec	102 sec	27 sec	177 sec	32 sec	193 sec
<b>1x 10<sup>11</sup> ions/cm<sup>2</sup></b>	10 sec	66 sec	29 sec	163 sec	28 sec	175 sec
<b>1x 10<sup>12</sup> ions/cm<sup>2</sup></b>	11 sec	124 sec	27 sec	277 sec	35 sec	347 sec
<b>1x 10<sup>13</sup> ions/cm<sup>2</sup></b>	7 sec	66 sec	9 sec	88 sec	8 sec	88 sec

Thus, metal oxide based gas sensors are based on chemisorbed reactions on solid surfaces where reactive gases change physiochemical parameters such as crystallinity, grain size, type of conductivity and density of particles. Energy loss of SHI in electronic system of target introduces surface modification in target material. When this energy is transferred to lattice atom, there is huge change in temperature along the trajectory of ions. This increase in temperature is due to thermalization and heat exchange between defects. Formation of new bonds and defects are main mechanisms responsible for change in physical properties during cooling down process. Due to thermal spike process as describe earlier, strain generated in ZnO grains leads to fragmentation

of grains into smaller grains with increased ion fluences. Nano-crystalline ZnO thin film based hydrogen sensor shows maximum sensitivity of 89.84 % at  $1 \times 10^{12}$  ions/cm<sup>2</sup> at 175 °C operating temperature.

## 8.8 CONCLUSION

This chapter investigate effects of post deposition treatment such as swift heavy ion (SHI) on hydrogen sensors relative response. SHI irradiation plays an important role in the enhancement of hydrogen sensitivity as it modifies structural, optical, surface morphology of RF sputtered ZnO thin films. Hydrogen response were measured on ZnO thin films which exposed to 120 MeV Au<sup>+9</sup> ions with various ion fluences varies from  $1 \times 10^{11}$  ions/cm<sup>2</sup> to  $1 \times 10^{13}$  ions/cm<sup>2</sup>. Un-irradiated ZnO thin films were high crystalline with hexagonal wurtzite structure and have high in-plane compressive stress (-1.78 GPa) which conformed by XRD. Although at  $1 \times 10^{13}$  ions/cm<sup>2</sup> fluence, ZnO thin film becomes almost stress free but its crystallinity decreases from pristine ZnO thin film. CL spectroscopy indicates an optical band gap enlargement, likely correlated with stress decrease.

Due to SHI irradiation, grain fragmentation reduces average grain size and increases its surface roughness as ion fluences increase. Average grain size reduction enhances the surface reaction area for hydrogen gas, which increases gas sensor relative response. It was observed that the gas sensor's sensitivity is strongly dependent on ion fluences and operating temperature. Nano- crystalline ZnO thin film based hydrogen sensor gives highest sensitivity of 89.84% and fast response time ~34.67 sec with moderate fluence ( $1 \times 10^{12}$  ions/cm<sup>2</sup>) at 175 °C operating temperature.

...

